on the same basis as the proof of (16). Therefore, $A^0=B^0\approx 0$ and expression (B3) is reduced to

$$\langle \Delta A \Delta a + \Delta B \Delta b \rangle, \tag{B4}$$

where we have also used $\langle a^0 \Delta A \rangle = \langle b^0 \Delta B \rangle = 0$. ΔA and ΔB are functions of $\delta_{l'}{}^{J'}$ while Δa and Δb refer only to $\delta_l{}^J$. For $l \neq l'$ and/or $J \neq J'$, the fluctuation over the averaging interval in functions of $\delta_l{}^J$ are assumed uncorrelated to those in functions of $\delta_{l'}{}^{J'}$; thus, expression (B4) is equal to zero, and we have proved Eq. (17) for this case.

For $J=J'$ and $l=l'$ the left-hand side of Eq. (17) reduces to

$$\left\langle \sigma_{rl'}{}^{J'} \begin{Bmatrix} 2\sin^2\delta_{l'}{}^{J'} \\ \mathfrak{F} \sin 2\delta_{l'}{}^{J'} \end{Bmatrix} \right\rangle,$$

and we may use the result proved in Ref. 7,

$$\left\langle \sigma_{rl'}{}^{J'} \begin{Bmatrix} 2\sin^2\delta_{l'}{}^{J'} \\ \mathfrak{F} \sin 2\delta_{l'}{}^{J'} \end{Bmatrix} \right\rangle \approx \begin{Bmatrix} \langle \sigma_{rl'}{}^{J'} \rangle \\ 0 \end{Bmatrix} \tag{15}$$

which completes the proof of Eq. (17).

PHYSICAL REVIEW VOLUME 131, NUMBER 4 15 AUGUST 1963

Quasifree Proton-Neutron and Proton-Proton Scattering at 140 MeV*

J. LEFRANÇOIS,† R. A. HOFFMAN,‡ E. H. THORNDIKE,§ AND RICHARD WILSON
Cyclotron Laboratory, Harvard University, Cambridge, Massachusetts
(Received 27 March 1963)

Measurements of the neutron-proton triple scattering parameters R and A have been performed by scattering a polarized proton beam on a deuterium target. Quasifree proton-neutron events were separated by requiring a time coincidence between the scattered proton and the recoil neutron. The quasifree results were corrected by the method of Cromer and Thorndike (second following paper) to give the following equivalent free neutron-proton results:

$\theta_{c.m.}$	R	A
42°	+0.169±0.100	−0.020±0.089
52½°	+0.080±0.093	+0.070±0.074
63°	−0.023±0.073	+0.210±0.088
73½°	−0.151±0.095	+0.125±0.105
83½°	−0.146±0.210	+0.532±0.220

Measurements were also made requiring a coincidence between the scattered proton and a recoil proton. In this manner, the R and A parameters for quasifree proton-proton scattering in deuterium were obtained. The results are

$\theta_{c.m.}$	R	A
65½°	−0.246±0.061	−0.229±0.087
73½°	−0.273±0.064	−0.144±0.069
83½°	−0.050±0.125	+0.016±0.133

The free n-p values agree with the predictions of the Yale phase-shift solutions YLAN 3 and 3M. The quasifree p-p values agree with free p-p measurements.

I. INTRODUCTION

In recent years the proton-proton interaction has been studied with some vigor. Near 140 MeV, the cross section,[1] polarization,[1] and triple-scattering parameters[2–4] D, R, and A, have been measured. Similar programs have been carried out near 210 [5] and 315 MeV.[6] Phase-shift analyses performed on these measurements indicate that the p-p scattering matrix has been very nearly determined.[7]

* Supported by the joint program of the U. S. Office of Naval Research and the U. S. Atomic Energy Commission. A preliminary report on part of this work has been previously published [Phys. Rev. **125**, 973 (1962)]. The results quoted in the present article differ slightly from those in the preliminary report, and supercede them.

† Present address: Laboratoire des Hautes Energies, Orsay, France.

‡ Present address: Department of Physics, Union College, Schenectady, New York.

§ Present address: Department of Physics, University of Rochester, Rochester, New York.

[1] J. N. Palmieri, A. M. Cormack, N. F. Ramsey, and Richard Wilson, Ann. Phys. (N. Y.) **5**, 229 (1958).

[2] C. F. Hwang, T. R. Ophel, E. H. Thorndike, and Richard Wilson, Phys. Rev. **119**, 352 (1960).

[3] E. H. Thorndike, J. Lefrançois, and Richard Wilson, Phys. Rev. **120**, 1819 (1960).

[4] S. Hee and E. H. Thorndike (to be published).

[5] A. C. England, W. A. Gibson, K. Gotow, E. Heer, and J. Tinlot, Phys. Rev. **124**, 561; J. H. Tinlot and R. E. Warner, *ibid.* **124**, 890 (1961); K. Gotow, F. Lobkowicz, and E. Heer, *ibid.* **127**, 2206 (1962).

[6] J. E. Simmons, Phys. Rev. **104**, 416 (1956); O. Chamberlain, E. Segré, R. D. Tripp, C. Wiegand, and T. Ypsilantis, *ibid.* **105**, 288 (1957).

[7] G. Breit, M. H. Hull, Jr., K. E. Lassila, and K. D. Pyatt, Jr., Phys. Rev. **120**, 2227 (1960).

Neutron-proton scattering has been less thoroughly studied. This fact is due to the nonexistence of useable pure neutron targets, and to the inferior properties of neutron beams as compared to proton beams.

Two methods have been used for studying the n-p interaction. The direct method, that of scattering a neutron beam by a proton target, suffers from the inferior properties of neutron beams. It has been used to measure cross sections and polarizations,[8] and recently, triple-scattering parameters.[9]

The second method consists of scattering a proton beam from a target containing neutrons, in particular, from deuterium. Proton-deuteron scattering is the simplest kind of proton-nucleus scattering, since the deuteron contains but two nucleons, which are very loosely bound. As such, one hopes to be able to describe proton-deuteron scattering in terms of nucleon-nucleon scattering amplitudes. If the nucleon-nucleon amplitudes were known, the theoretical descriptions of proton-deuteron scattering could be checked by experiments. Alternatively, if the theoretical descriptions were trusted, proton-deuteron scattering experiments could be used to obtain nucleon-nucleon scattering amplitudes. In fact, the theoretical descriptions are approximations, and the nucleon-nucleon amplitudes (particularly n-p amplitudes) are only approximately known. The research described in this and the following two papers aims at improving both situations.

The first subsequent paper[10] (hereafter referred to as II) deals with elastic proton-deuteron scattering. The second subsequent paper[11] (hereafter referred to as III) gives a theoretical treatment of inelastic proton-deuteron scattering. This paper describes some experiments on inelastic scattering.

Inelastic p-d scattering can be qualitatively described by the spectator model. In this model, the incident proton interacts with only one of the two target nucleons. The other (spectator) particle retains the same momentum it had before the scattering event, as determined by the deuteron wave function. The incident and struck particles scatter as would two free nucleons with the same incident momenta.

Since these are three-body kinematics, in addition to the energy of the incident particle, one must specify 5 quantities to determine the final state kinematics. These are conveniently taken as the polar scattering angle of the incident particle, θ_2; the azimuthal scattering angle of the incident particle ϕ_2; the energy after scattering of the incident particle E_2; the polar scattering angle of the struck or recoil particle θ_r; and the azimuthal scattering angle of the recoil particle ϕ_r. These serve to determine, through the conservation of momentum and energy, the energy of the recoil particle E_r, and the direction and energy of the spectator particle θ_s, ϕ_s, E_s. These relations are, of course, valid quite independently of the spectator model.

The spectator model predicts that cross sections shall peak at those angles and energies corresponding to free nucleon-nucleon kinematics. Thus, for $\phi_2=0$, and θ_2 fixed, the cross section peaks when the included angle between scattered and recoil particle is approximately equal to 87°, with a half-width of $\Delta\theta_r=\pm 6°$; it peaks when E_2 is approximately equal to $E_0\cos^2\theta_2$, with a half-width of $\Delta E_2=\pm 7$ MeV. (These nonzero half-widths are due to the momentum distribution of the nucleons in the deuteron.)

Usually the spectator particle energy is $\lesssim 6$ MeV, and, hence, lower than both E_2 and E_r. Thus, if one observes experimentally a high-energy proton scattered into θ_2, and a high-energy neutron scattered roughly 87° away, the spectator model would predict that the scattering event would have the properties of an n-p scattering. We call such an event a quasifree p-n scattering. Similarly, a quasifree p-p scattering event is one whose kinematics approximate free p-p scattering. Corrections to the spectator model, which enable one to relate quasifree parameters to free parameters, are discussed in III. These corrections are frequently large, and *cannot be ignored.*

The cross section and polarization in quasifree scattering of protons on deuterium have already been measured[12]; the present article describes the measurement of the triple-scattering parameters R and A in quasifree proton-neutron and proton-proton scattering in deuterium.

The A and R parameters introduced by Wolfenstein[13] relate the polarization of the scattered proton, in the plane of scattering and normal to the direction of motion, to the polarization of the incident proton along the direction of motion (in the case of A) or normal to the direction of motion and in the plane of scattering (in the case of R).

In the next section (Sec. II) the experimental apparatus is described. In Sec. III the procedure of performing the measurements is discussed. The experimental results are summarized in Sec. IV, and in Sec. V the interpretation of the results and corrections to them are taken up.

II. EXPERIMENTAL APPARATUS

General

The experimental arrangement is shown in Fig. 1. Most of the apparatus is similar to that used in the measurement of R in free p-p scattering.[3] A proton beam

[8] For a summary of experiments, see M. H. MacGregor, M. J. Moravcsik, and H. P. Stapp, Ann. Rev. Nucl. Sci. **10**, 324 (1960).

[9] P. M. Patel, A. Carroll, N. Strax, and D. Miller, Phys. Rev. Letters **8**, 491 (1962).

[10] R. A. Hoffman, J. Lefrançois, and E. H. Thorndike, following paper, Phys. Rev. **131**, 1671 (1963).

[11] A. H. Cromer and E. H. Thorndike, second following paper, Phys. Rev. **131**, 1680 (1963).

[12] A. F. Kuckes and Richard Wilson, Phys. Rev. **121**, 1226 (1961); A. Kuckes, R. Wilson, and P. F. Cooper, Jr., Ann. Phys. (N. Y.) **15**, 193 (1961).

[13] L. Wolfenstein, Ann. Rev. Nucl. Sci. **6**, 43 (1956).

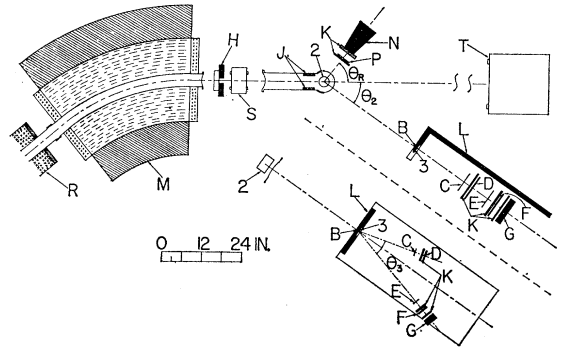

FIG. 1. Scale drawing of the experimental arrangement showing: (2) hydrogen target; (3) analyzing scatterer; (B,C,D,E,F,G,N,P) scintillation counters; (H) main defining slits; (J) antiscattering slits; (K) copper absorbers; (L) iron shielding; (S) ion chamber; (T) Faraday cup; (M) bending magnet, used in the A measurement; and (R) solenoid magnet.

initially polarized in the vertical plane passes through a solenoid magnet (R) in which the polarization of the beam precesses by 90° around the direction of motion. On leaving the solenoid the polarization is in the horizontal plane and normal to the direction of motion; in the experiment measuring R the beam then struck the liquid-deuterium target (2). In the experiment measuring A a bending magnet (M) was inserted between the solenoid and the target; because of the anomalous magnetic moment of the proton the spin precesses at a higher rate than the proton's momentum, so that at the exit of the magnet (M) the spin was along the direction of motion of the proton.

Protons scattered from the deuterium through an angle θ_2 in the horizontal plane are detected by the scintillation counter B and strike the analyzing scatterer (3). Protons scattering here through an angle θ_3 in the vertical plane are detected by the counter-telescopes CD or EFG. Counter P detects recoil protons from the deuterium scattering and counter N detects recoil neutrons.

The sign of the incident polarization may be reversed by reversing the current direction in the solenoid. We denote the two directions by N (normal) and R (reversed). The angles θ_3 may also be reversed; the two positions are denoted U (up) and D (down). If I_{km} is the counting rate for a θ_3 direction k and solenoid current direction m, the asymmetry e_{3s} is given by

$$e_{3s}=\frac{I_{DN}+I_{UR}-I_{UN}-I_{DR}}{I_{DN}+I_{UR}+I_{UN}+I_{DR}}. \quad (1)$$

The product P_1P_3 of the incident polarization (P_1) and of the analyzing power of the third scatterer (P_3) is measured by performing a double scattering experiment ($\theta_2=0$) with the magnet (M) removed. If the same sign convention as in Eq. (1) is used to define P_1P_3, then

$$e_{3s}=RP_1P_3, \quad \text{or} \quad e_{3s}=-AP_1P_3. \quad (2)$$

The minus sign in the expression for A arises from the choice of direction of bend of the magnet (M).

As has been discussed previously,[3] the reversal of incident polarization by means of the solenoid as well as the reversal of θ_3 angles causes many spurious asymmetries to cancel.

The Beam

The beam used for the experiment was the polarized proton beam of the Harvard synchrocyclotron.[14] The beam energy was approximately 142 MeV and its polarization was roughly 60%.

The solenoid current was adjusted to cause the polarization to precess 91° (the desired value is 90°) and was regulated to within 1%. For the A experiment the bending magnet current was adjusted to bend the beam through an angle of (43.6±1.5°) and was regulated to within 0.3%. With this angle of bend the polarization of the beam would precess to within 4.5° of parallel to its momentum; the remaining transverse polarization was later measured and corrected for.

After passing through the magnets, the beam was defined by the slits (H). For the R experiment the slit opening was $1\frac{1}{2}$ in. wide by 2 in. high; there was a systematic energy dispersion at the slits of 5±2 MeV/in. in the horizontal plane and the mean energy at the center of the D_2 target was 140±1 MeV.

For the A experiment the slit opening was $1\frac{1}{4}$ in. wide by 2 in. high; the bending magnet virtually eliminated the systematic energy dispersion and the mean energy at the center of the D_2 target was now $137\frac{1}{2}$±1 MeV.

As discussed by Thorndike *et al.*,[3] the solenoid magnet had the undesired effect of changing the beam intensity distribution at the slits, resulting in a change in the zero position of the analyzing scattering angle θ_3. To compensate for this effect a small horizontal magnetic field perpendicular to the direction of the beam was applied to the beam before it entered the solenoid. The direction of this field was reversed when the solenoid current was reversed and the value of the field was adjusted to cancel the variation in θ_3 zero position with solenoid current direction.

The Target and the Scattering Tables

The liquid-D_2 target system was similar to a system designed by Postma[15] and is described at length by Hoffman.[16] The target cell was $2\frac{7}{8}$ in. in diameter and had walls of 2 mil-beryllium copper. The entrance window of the vacuum jacket was made of 2-mil Mylar and the exit window was of 7-mil Mylar.

[14] G. Calame, P. F. Cooper, Jr., S. Engelsberg, G. L. Gerstein, A. M. Koehler, A. Kuckes, J. W. Meadows, K. Strauch, and R. Wilson, Nucl. Instr. **1**, 169 (1957).

[15] H. Postma and Richard Wilson, Phys. Rev. **121**, 1229 (1961).

[16] R. A. Hoffman, thesis, Harvard University, 1961 (unpublished).

The main scattering table was the table already used in the measurement of R_{p-p}[3]. The table pivoted in a ball and socket beneath the D_2 target. The counter telescopes CD and EFG were attached to arms which pivoted in a vertical plane around an axis aligned with the center of the analyzing scatterer. Each telescope was constrained in two ways. A point near the scintillator was pinned to a sine bar, the other end of which was pinned to a point whose distance above the horizontal plane could be adjusted.

The zero position of θ_3 was set by this adjustment, and the angle θ_3 by the distance between the two pins. Two leveling screws at the base of each telescope assembly were used to adjust the horizontal position of the telescopes and to level them.

The arm supporting the recoil counters was supported at one end by a ball pivot which rested in a cup attached to the main table. With the help of a plumb bob the cup was centered directly over the main table θ_2 pivot. The other end of the recoil arm was supported by two leveling screws resting on an aluminum table. The P and N counters could be moved along the arm to adjust their distances from the pivot and were bolted down at the appropriate places. The P counter distance was varied between 9 and $10\frac{1}{2}$ in. from the target. The N counter front plate was always $1\frac{1}{2}$ in. behind the P counter. The distances were chosen so that approximately $\frac{1}{4}$ to $\frac{1}{3}$ of the recoil particles passed through the counters.

The Carbon Scatterer and the Counters

The analyzing scatterer (3) was placed behind counter B. It was a block of carbon $2\frac{3}{4}$ in. high, 3 in. wide. The thickness was

$\frac{1}{2}$ in. when $\theta_2=20°, 25°, 30°$;

$\frac{3}{8}$ in. when $\theta_2=35°$; and

$\frac{1}{4}$ in. when $\theta_2=40°$.

The counters B, C, D, E, F, G, P were made of Pilot B plastic scintillator connected by short light pipes to 6810-A phototubes. The scintillator dimensions and the distances from the counters to the targets are given in Table I.

TABLE I. Scintillator dimensions and distances between counters and pivots.

Counter	Scintillator height (in.)	Scintillator width (in.)	Scintillator thickness (in.)	Distance from center of counter to θ_2 or θ_3 pivot
B	2	2	$\frac{3}{32}$	34 in. from θ_2
C	2	6	$\frac{1}{8}$	$18\frac{1}{4}$ in. from θ_3
D	$3\frac{3}{8}$	8	$\frac{5}{16}$	$21\frac{1}{4}$ in. from θ_3
E	2	6	$\frac{1}{8}$	26 in. from θ_3
F	$3\frac{3}{8}$	8	$\frac{5}{16}$	29 in. from θ_3
G	$3\frac{1}{2}$	8	2	$32\frac{1}{2}$ in. from θ_3
P	4 in. diam		$\frac{1}{8}$	9 in. from θ_2 ($10\frac{1}{2}$ in. when $\theta_2=40°$)
N	Truncated cone: half-angle of 6°; diam 3.8 to 6 in.		9	17 in. from θ_2 ($18\frac{1}{2}$ in. when $\theta_2=40°$)

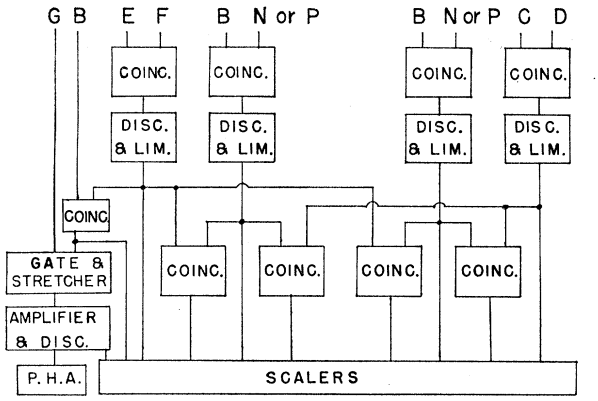

FIG. 2. Block diagram of the electronic circuitry.

Counter B was the defining counter for the θ_2 angle. The counters C and E defined the scattering angle θ_3. Counters D and F together with copper absorbers (K) were used to discriminate against low-energy particles. The absorber thicknesses used were sufficient to stop 5 to 10% of the protons from quasifree p-p or quasifree p-n events. Counter G, in which the scattered protons were stopped, was used to separate by pulse-height analysis protons elastically scattered from deuterium. (The use of this counter is discussed in II.)

The P counter placed at a recoil angle $\theta_r=86°-\theta_2$ detected recoil protons produced by quasifree events in deuterium. Copper absorber (K) placed in front of the counter prevented deuterons from being detected.

The neutron counter (N) was a plastic scintillator block in the form of a truncated cone, the axis of which was parallel to the path of the recoil particles. The half-angle of the cone was 6°, the diameter of the base was 6 in. and the length was 9 in. The plastic scintillator was separated by a $\frac{1}{4}$-in. air gap from a Lucite lightpipe glued onto the face of a 5-in.-diameter RCA 7046 phototube. The absorber in front of N prevented charged particles from entering the neutron counter.

Electronic Circuitry

The output pulses from counters C, D, E, and F were fed directly to a coincidence circuit (described in Ref. 17). The pulses from counters B and P were first shortened by clipping lines 0.5-m long. The output pulses from the neutron counter were sent to an avalanche transistor discriminator which gave 4-nsec output pulses of uniform height. The resolving times for BP or BN coincidences were about 3.5 nsec, for CD or EF coincidences about 7 nsec. A block diagram of the electronic circuitry is shown in Fig. 2.

Random coincidences were measured by delaying the appropriate signal by a period of the cyclotron rf (44 nsec). The highest random coincidence rates were between events in P or N and BCD or BEF events.

These rates varied from 10 to 20% of the real coincidence rate. On some occasions it was necessary to reduce the intensity of the incident beam to keep randoms from exceeding 20%. Two of the coincidence circuits were used to measure simultaneously BN prompt coincidences and either BN delayed coincidences ($\frac{1}{3}$ of the time), BP prompt coincidences ($\frac{1}{2}$ of the time) or BP delayed coincidences ($\frac{1}{6}$ of the time). It should be noted that nearly all of these random coincidences are the result of simultaneous events occurring in the deuterium target and cannot be prevented by shielding.

The only other non-negligible random rates were NB or PB in random coincidence with CD or EF. They were of the order of 1% or less and were either measured or calculated from the known NB, PB, CD, and EF rates.

Monitoring

Two beam monitors were used. The primary monitor was a Faraday cup (T) located 13 ft beyond the deuterium target. An ionization chamber (S) located just after the main slits (H) served as a secondary monitor (see Fig. 1). The ratio of the two monitors depended on the solenoid current direction; the variation was as high as 7% from N to R on some occasions. This dependence was attributed to a change in scattering from the main slits into the ionization chamber or to small movements of the beam at the Faraday cup. When averaged over solenoid directions the variation of the ratio of the two monitors is usually smaller than 2% and exhibits a slight dependence on the intensity of the beam. Errors caused by the monitoring system were always less than 0.004 in R or A.

III. EXPERIMENTAL PROCEDURE

Set-Up and Alignment

For the A measurement, the bending magnet was aligned so that the central portion of the beam was deviated within 1° of $43\frac{1}{2}$°, the deviation of this part of the beam being measured with x-ray film.

For both the A and R measurements, the slits, target, monitors, and scattering tables were aligned so that the only remaining significant misalignment was the shift in the $\theta_3=0°$ position when the solenoid was reversed.

The angle $(\theta_2+\theta_r)$ between the main scattering table and the recoil arm was set at each θ_2 by sweeping the recoil arm by 2° steps through the expected optimum region and measuring the rates of $NBEF$ and $PBEF$ coincidences; the angle used was that which gave the maximum $NBEF$ rate (corrected for randoms). For all θ_2, the angle $(\theta_2+\theta_r)$ used was $86°\pm\frac{1}{2}°$. The maxima for $PBEF$ coincidences were at the same recoil angles except for $\theta_2=30°$ where not all the recoil protons had sufficient energy to escape from the target.

It is also important to maintain the vertical position of the recoil arm, for vertical shifts in the positions of the recoil counters affected the $\theta_3=0°$ position. The recoil arm was kept level within limits such that the maximum effect upon the $\theta_3=0°$ position would be well under 0.01°.

Except for the neutron counter N, all the electronic apparatus was adjusted to operate on suitably wide plateaus. The neutron counter high voltage V_N was selected at each θ_2 by studying the $NBEF$ total and random coincidence rates as a function of V_N. The final choice of V_N was a compromise between three conflicting requirements: the counting rate for real events should be as high as possible and varying slowly with V_N; the relative random rate should be as low as possible; the energy threshold should be high enough to reject most of the "spectator" neutrons. The energy thresholds used are listed in Table III. The neutron counter energy thresholds were calibrated before each run with the aid of a Co^{60} γ source. After the gain of the phototube had been determined as a function of V_N, the counting rates of the Compton electrons were measured as a function of V_N, so the threshold for the Compton electrons could be found. Assuming a linear response of the scintillator to electron energies and taking into account the difference in energy between protons and electrons which give the same pulse height in the scintillator, the threshold energy for protons as a function of V_N could be determined.

The change in the $\theta_3=0°$ position of the telescopes upon reversing the solenoid current direction is due to electromagnetic effects in the solenoid and in the R experiment also to nuclear effects such as the variation of p-p, p-n, or p-d cross sections with energy coupled with the energy dispersion across the slits or polarization effects proportional to P_2. These effects are discussed in more detail elsewhere.[3,16,17]

The error in e_{3s} produced by a θ_3 misalignment is very nearly[18]

$$\Delta\epsilon=M\left(\frac{1}{\sigma}\frac{d\sigma}{d\theta}\right)_{15°}. \tag{3}$$

M, the first moment of the twice scattered beam, equals $\int A(\theta_3)\theta_3 d\theta_3$, where $A(\theta_3)$ is the normalized counting rate when the telescope is positioned at θ_3. $[(1/\sigma)(d\sigma/d\theta)]_{15°}$ is the fractional change per degree in the counting rate between $\theta_3=14°$ and $\theta_3=16°$, the angle used in the e_{3s} measurement being $\theta_3=15°$.

The counters were aligned roughly ($\pm0.05°$) with the solenoid off by requiring equal counting rates at 2 angles (U 3° and D 3° for the EF telescope; U 4° and D 4° for the CD telescope). The change in alignment due to the change in solenoid current was then measured by sweeping the counter telescopes through small θ_3 angles in one degree steps; $NBEF$, $PBEF$, BEF, $BEFG$, $NBCD$, $PBCD$, and, on some occasions, random coincidences were recorded. The first moment was approxi-

[17] J. G. J. Lefrançois, thesis, Harvard University, 1961 (unpublished).

[18] E. H. Thorndike, thesis, Harvard University, 1960 (unpublished).

mated by

$$\Delta\theta_0=\sum_{-n}^{+n} A(\theta_{3i})\theta_{3i}. \quad (4)$$

For the CD telescope $n=9$; for the EF telescope $n=7$. The magnitude of the sum is smaller than the magnitude of the integral by less than 3%.

The misalignment was measured again after the e_{3s} measurement. In this case the measurements were taken only at 4 up and 4 down values of θ_3, and the misalignment was given by

$$\Delta\theta_s(\theta_i)=\frac{2[A(\theta_i,U)-A(\theta_i,D)]}{A(\theta_{i-1},U)+A(\theta_{i-1},D)-A(\theta_{i+1},U)-A(\theta_{i+1},D)}, \quad (5)$$

or by

$$\Delta\theta_s'(\theta_i)=\frac{\pm[A(\theta_i,U)-A(\theta_i,D)]}{A(\theta_i,U)+A(\theta_i,D)-A(\theta_{i\pm1},U)-A(\theta_{i\pm1},D)}, \quad (6)$$

whenever $A(\theta_{i\pm1})$ were not both measured; $\Delta\theta_0$ was then approximated by an average, $\Delta\theta_{\rm av}$, of $\Delta\theta_s(\theta_i)$ and $\Delta\theta_s'(\theta_i)$ over the four angles used in the measurement. These angles were 2°, 3°, 4°, 5° for the EF telescope and 3°, 4°, 5°, 6°, for the CD telescope. This method was used only to correct for drift in the misalignment during the e_{3s} measurement. Since the correction was given by a comparison of $\Delta\theta_{\rm av}$ before and after the e_{3s} measurement it is believed that systematic differences between $\Delta\theta_0$ and $\Delta\theta_{\rm av}$ would cause an error of less than 0.01° in the determination of $\Delta\theta_0$.

At a given θ_3, measurements were taken for both solenoid directions without moving the counters; thus the N to R difference in $\Delta\theta_0$ would not be influenced, in a first approximation, by small mechanical errors like imperfect leveling of the counters, torsion of the sine bar, etc.

Errors in the $(\Delta\theta_{0N}-\Delta\theta_{0R})$ measurements caused by the facts that random coincidences were not always measured simultaneously and that the asymmetry measurement was done at an energy slightly different from that of the alignment (because of different energy losses in the carbon scatterer) were found to be smaller than 0.01°, giving rise to errors in R or A of less than 0.008.

Asymmetry and Background Measurements

The e_{3s} asymmetry was measured by reversing the solenoid current roughly every 30 min (every 6×10^{10} protons). The θ_3 angles were reversed roughly every 6 h. Every 12 h the circuit used to measure NB coincidences was interchanged with the circuit previously used to measure random NB coincidences. In this way differences in dead times or resolving times of the circuits would cancel out. At the end of the asymmetry measurement the θ_3 alignment was checked as described above.

The target was then emptied and the magnitude of the background was measured with θ_3 set equal to 0°. Copper absorbers in the CD and EF telescopes were increased to compensate for the change in energy of the scattered particles due to the absence of deuterium in the target. The rate of PB or NB coincidences was found to be roughly 0.4% of the rate with deuterium in the target.

Because the background events are also quasifree p-p or p-n events the scattered proton has roughly the same energy as in the quasifree p-p and p-n reaction in deuterium; thus the maximum asymmetry of the background would be P_1P_3 (if R or $A=1$). This fact was used to calculate the maximum possible error in R or A due to the fact that we did not measure the asymmetry of the background; the error in R or A was found to be less than 0.004.

P_1P_3 Measurement

P_3, the analyzing power of carbon, depends strongly on energy. In order to measure P_1P_3 one has to obtain a proton beam, of polarization P_1 in the horizontal plane, with an energy spectrum identical to the energy spectrum of protons scattered in quasifree collisions on deuterium. Thus at the end of the run, θ_2 was set to 0° and the energy of the beam was lowered by lead absorbers placed after the main slits (H). The energy spread was increased by placing in the beam a brass absorber made of rods of triangular cross section, $\frac{3}{8}$ in. wide, roughly $\frac{3}{8}$ in. thick, and 4 in. long, placed side by side and glued on an aluminum plate. The difference in the thickness of brass from point to point resulted in an energy spread. The maximum thickness of the brass was chosen such that a range curve taken with this beam would have the same shape as that taken with protons scattered in quasifree events. Errors coming from differences between these shapes were calculated from known values of P_1P_3 as a function of energy for monoenergetic beams.

The beam intensity was reduced until the electronic circuitry was functioning properly. For such a small beam intensity the Faraday cup could not be used any more as a monitor. Instead, the B rate was used as a monitor. Special 30 Mc/sec scales-of-4 (described in Ref. 17) were used to scale B with small counting losses (4% or less). At the beginning of the measurement a range curve was taken, and the CD and EF counters were aligned. The $\Delta\theta_{0N}-\Delta\theta_{0R}$ misalignment was measured by setting θ_3 at 2 angles (3°, 4° for the EF telescope; 4°, 5° for the CD telescope) on each side of $\theta_3=0°$. P_1P_3 was then measured. Following this measurement the fractional difference in counting rate between 14° and 16°, was measured with the solenoid turned off.

For these measurements, the copper absorber placed in the CD and EF telescopes was the same as that used in the e_{3s} measurement.

At this time the energy of the direct beam was also determined by range curves taken with varied amounts of copper absorber placed in front of the F counter.

IV. ANALYSIS AND RESULTS

Corrected Asymmetries

The random coincidences between N or P and BCD or BEF were subtracted from the total coincidences $NBCD$, $NBEF$, $PBCD$, and $PBEF$ measured with $\theta_3=15°$. e_{3s} was calculated for the corrected counts. The statistical error on the asymmetry was calculated from the total number of counts collected and from the number of random events. The change in asymmetry which would result from a 10% increase or decrease of all random coincidences was also calculated. The change was combined with the "counting statistics" error. We thus took into account the possibility that our technique of measuring random coincidences gave us an erroneously high or low value for the random rate. The change was always less than 0.002 in the asymmetry measurement.

The Misalignment Correction

$$\Delta\epsilon=-\frac{1}{\sigma}\frac{d\sigma}{d\theta}\left(\frac{\Delta\theta_{0N}-\Delta\theta_{0R}}{2}\right) \tag{7}$$

was added to the asymmetry. The value of $\Delta\theta_0$ was calculated as described earlier.

The error attached to the misalignment correction came from 4 different sources. These four errors were combined quadratically to form the misalignment errors. First, there was an error on $\Delta\theta_0$ from counting statistics, which amounted to as much as 0.04° in some cases. Secondly, an error equal to $\frac{1}{3}$ the difference between $\Delta\theta_{av}$ before and after e_{3s} accounted for our uncertainty on $\Delta\theta_0$ due to the drift. Thirdly, an error equal to 10% of $(\Delta\theta_{0N}-\Delta\theta_{0R})$, or 0.02°, whichever was bigger, included dead time effects, monitoring differences, small movements of the beam, approximation in the measurement of the profile by discrete points, change in $\Delta\theta_0$ with energy cutoff, etc. Finally, a fourth error was included because of the uncertainty in the value of $(1/\sigma)d\sigma/d\theta$. This uncertainty was simply a "counting statistics" error in the measurement described earlier. Corrections for the fact that the slope was measured with $\theta_2=0°$ with an artificially produced energy spread were always found to be negligible. The misalignment corrections ranged from +0.010 to −0.017 in e_{3s}; the error in these corrections ranged from 0.001 to 0.005 in e_{3s}.

After correction for misalignment, the asymmetries for the CD and EF telescopes were combined, weighting each by the square of the reciprocal of the combined statistical and misalignment errors. The background errors were then included.

TABLE II. Values used for P_1P_3.

θ_2 (lab)		R measurement	A measurement
20°		0.189±0.010	−0.187±0.022
25°		0.150±0.009	−0.151±0.017
30°	p-n	0.103±0.007	−0.101±0.014
	p-p	0.082±0.008	−0.080±0.014
35°	p-n	0.071±0.007	−0.068±0.010
	p-p	0.068±0.007	−0.066±0.011
40°	p-n	0.051±0.008	−0.048±0.009
	p-p	0.050±0.007	−0.050±0.009

P_1P_3

P_1P_3 was calculated from the BCD and BEF triple coincidence rates. Misalignment corrections were applied as for e_{3s}. The results from the two counter telescopes were combined with equal weighting to cancel out monitoring errors. The main source of error in P_1P_3 was the counting statistics error; errors arising from the difference between the artificially produced energy spread and the spectrum produced by quasifree scattering in deuterium was less than half as large as that produced by counting statistics alone. An additional error of 10% of P_1P_3 was included in the case of the A experiment to include possible differences in P_1 between the e_{3s} and P_1P_3 measurements. This error was not included for R because the e_{3s} and P_1P_3 measurements were made during the same runs in that case. The values of P_1P_3 used are listed in Table II.

Small Corrections and Errors

Because of the combined use of solenoid (i.e., incident polarization) reversal and θ_3 angle reversal, the only significant misalignment is the shift in the zero position of θ_3. Most mechanical misalignments such as nonlevelness of the scattering tables, torsion of the θ_3 sine bars, failure of the CD or EF counters to move in a vertical plane, produce errors which cancel upon reversing the solenoid. Some of these effects may not cancel completely if the levelness of the incident beam changes upon solenoid reversal, but since the direction of the incident beam does not change by more than $\frac{1}{4}°$ vertically, calculation showed that the maximum effect upon A or R was less than 1/20 the statistical error.

The ratio of the two monitors depended somewhat upon the solenoid current direction. It was also noticed during N counter calibration that the gain of the N counter was affected by the solenoid. During data collection it was observed that the NB and PB doubles rates varied with the solenoid current direction. All of these effects should cancel out upon reversal of the counter telescope positions. As a check "asymmetries" were calculated for the NB and PB rates and for the ratio of the monitors using Eq. (1). The down position was arbitrarily chosen to be that of the CD telescope. Since the EF telescope was at the same time in the up position and since the results for the two telescopes were combined in roughly a 2 to 1 ratio of CD to EF, the final

asymmetry would be changed by only one-third such spurious "asymmetries." At all angles it was found that such effects were less than 1/20 the final statistical error.

Transverse vertical polarization of the incident beam resulting from incorrect choice of solenoid current affects the final asymmetry only in conjunction with a change of levelness of the beam and thus changes A or R by less than 0.001.

In the R experiment, a longitudinal component of polarization of the incident beam will mix in A. A search was made for such longitudinal polarization and it was found to be small but dependent upon the main slit position. The values of A being known, the resulting errors were calculated and found to be less than one-eighth the statistical error in the worst case.

In the A experiment, an incorrect angle of bend of the beam in the magnet (M) results in some residual transverse horizontal polarization and hence mix in R. The angle of bend was measured photographically and transverse polarization was searched for by measuring the asymmetry with $\theta_2=0°$. The final values of A were corrected for the amount of R present; the largest correction was less than one-twelfth the statistical error in A and the uncertainties were of the same order of magnitude.

In the R experiment, the presence of an energy dispersion at the main slits (H) gives rise to a spurious positive asymmetry because of the variation of cross section of carbon with energy and angle. Because it depends only upon the properties of the scatterer the correction is the same for p-p and p-n events and is typically about 0.02 in R. An uncertainty of one-third the correction was included in the final error. No such corrections were made to A as the bending magnet appeared to eliminate the energy dispersion.

There is some experimental failure to identify correctly the product particles of scattering events. For example, the recoil proton of a quasifree p-p event may knock a neutron out of the absorber between the P and N counters so that the event is also detected falsely as a quasifree p-n event. At each θ_2 angle PNB coincidences were measured to evaluate this contamination and found to be less than 0.9% of the p-n rates at all angles, resulting in corrections of 0.002 or less to either A or R. Some further such events might occur if the recoil proton knocks a neutron out of the target so that no PNB coincidence will be formed, but calculation showed that fewer than 0.2% of the $NBCD$ or $NBEF$ counts came from this source. Conversely, a recoiling neutron might knock a proton out of the target or counters and cause the recording of a spurious p-p event. Calculation showed that fewer than 0.5% of the $PBCD$ or $PBEF$ events came from this source, producing corrections to A or R of 0.003 or less.

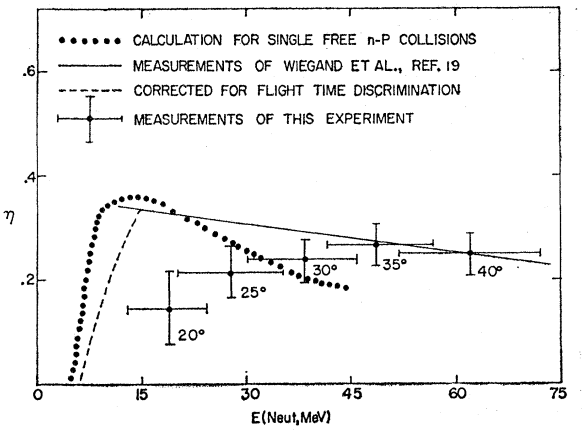

FIG. 3. Neutron counter efficiency η versus neutron energy. See text for fuller description of the curves and points.

TABLE III. Minimum energies with which particles can leave deuterium target and be detected.

θ_2 (lab)	Protons in D or F (MeV)	Protons in P (MeV)	Neutrons in N (MeV)
20°	106	···	4.1 (A)
			3.6 (R)
25°	94	···	4.1
30°	83	16	4.2 (A)
			4.3 (R, first run)
			3.6 (R, second run)
35°	72	21	4.2 (A)
			4.5 (R, first run)
			4.8 (R, second run)
40°	60	24	4.9 (A)
			5.4 (R)

Results: Acceptable Kinematics

The final experimental values of A and R obtained are listed in Table IV. As is discussed in III following, the corrections necessary to relate these values of the A and R parameters to those of free p-p and n-p scattering are large and cannot be ignored.

Since the kinematics of the quasifree events are not uniquely defined by the scattering angle θ_2, it is necessary to know what range of energies and recoil angles were accepted by the apparatus in order to interpret the results in terms of a model. Table III lists the minimum

TABLE IV. R and A for quasifree scattering.

θ_{lab}	R (quasifree)	A (quasifree)
	p-n Scattering	
20°	+0.029±0.080	+0.052±0.072
25°	−0.006±0.082	+0.123±0.059
30°	−0.061±0.063	+0.214±0.076
35°	−0.160±0.089	+0.098±0.095
40°	−0.164±0.207	+0.496±0.216
	p-p Scattering	
30°	−0.246±0.061	−0.229±0.087
35°	−0.273±0.064	−0.144±0.069
40°	−0.050±0.125	+0.016±0.133

energies which a proton would need upon emerging from the deuterium target if it were to be able to reach the P counter or the D or F counters. These threshold values were obtained by taking account of the energy losses in the copper absorbers (K, Fig. 1) used in front of the counters at each θ_2 angle. For the D and F counters the energy losses in the preceding counters and carbon scatterer were also considered.

It is also necessary that the neutron counter detection efficiency be known as a function of neutron energy. Some crude determinations of neutron detection efficiency were made as follows. For θ_2 angles of 30°, 35°, and 40°, the ratio of *NBEF* to *PBEF* coincidences should equal the ratio of the *n-p* to *p-p* cross sections times the neutron detection efficiency. At 20° and 25° where *PBEF* was not recorded, the efficiency was inferred (with less certainty) from the *NBEF* to *BEF* ratio. The results of these measurements are shown in Fig. 3. The vertical bars indicate the uncertainty in the efficiency determination. The horizontal bars indicate the range of neutron energies covered by the measurement.

The dotted curve shown in the figure gives the efficiency calculated assuming detection is due solely to single *n-p* collisions. The solid curve gives the experimental results of Wiegand *et al.*,[19] scaled to allow for the difference between their counter thickness (6 in.) and ours (9 in.). Below 12 MeV, the experimental results of Wiegand coincide with the dotted curve. Above 25 MeV, the inelastic events in the carbon of the neutron counter become important, and the measurements of Wiegand *et al.* differ appreciably from the calculations.

In order to make the curves comparable with the points from our experiment, the curves must be reduced at low energies, because here neutrons will be discriminated against because of their long flight time. The dashed curve shows the effect of this reduction.

Thus, one would expect our experimental points to agree with the dashed curve below 15 MeV, and the solid curve above 15 MeV. The agreement for the 30°, 35°, and 40° points is quite satisfactory. The 20° and 25° points are low. The cause of this substantial discrepancy is not known. The curves are based on neutron counters whose minimum dimension is the thickness. Our counter has the thickness as its maximum dimension. Perhaps neutrons are being scattered out of the sides of the counter by carbon, and hence lost. Perhaps the method of determining the efficiency from the *NBEF* to *BEF* ratio is in error, due to an inadequate inclusion of the effect of final state interactions on the quasifree *p-n* cross section. Kuckes and Wilson[12] also obtained an anomalously low neutron counter efficiency, calculating in a manner similar to ours.

Without doing violence either to the curve or to the experimental points, one can assume the efficiency is constant above 18 MeV, and drops linearly to zero somewhere between 5 and 9 MeV.

[19] C. E. Wiegand, T. Elioff, W. B. Johnson, L. B. Auerbach, J. Lach, and T. Ypsilantis, Rev. Sci. Instr. **33**, 526 (1962).

Consistency

The measurements of e_{3s} for both *p-p* and *p-n* scattering and of P_1P_3 from the CD telescope were compared with those from the EF telescope. For the A e_{3s} measurements, of eight comparisons, four differences were less than one standard deviation and none were greater than 1.6 standard deviations. For the R e_{3s} measurements, only one out of twelve comparisons showed a difference of greater than one standard deviation and none differed by more than two standard deviations. For P_1P_3, six out of eighteen measurements differed by more than one standard deviation and two differed by 2.6 and 2.1 standard deviations, respectively; these two measurements of P_1P_3 were for a monoenergetic beam and so did not enter into the results directly.

Data for the R measurements at $\theta_2=30°$ and 35° were collected during two runs and the results from the first runs were compared with those from the second; three of the four comparisons differed by less than one standard deviation, the other by 1.3 standard deviations.

For the A e_{3s} measurements, the measurements made by each counter telescope through the two different coincidence circuit channels were compared; nine of the sixteen comparisons differed by less than one standard deviation and none differed by more than 1.8 standard deviations. Thus, the internal consistency of the data appears to be quite satisfactory.

V. INTERPRETATION OF RESULTS

Scattering Energy and Angle

The kinematical relations in quasifree *p-p* or *p-n* scattering in deuterium, though similar to those in free nucleon-nucleon scattering, are three-body kinematics and, hence, a knowledge of the polar and azimuthal angle of scattered and recoil particles and the energy of the scattered particle is needed to specify the momenta of all particles for a given incident particle momentum. These kinematical relations have been previously discussed by Kuckes and Wilson.[12] It is sufficient to say here that if the momenta are known it is possible to

TABLE V. Laboratory scattering energy and center-of-mass scattering angle, and their rms variations, for equivalent free *n-p* events.

θ_{lab}	$\theta_{c.m.}$	$\Delta\theta_{c.m.}$	E^a (MeV)	ΔE (MeV)
20°	42.1°	3.6°	137½	7.5
25°	52.5°	3.7°	137½	8.0
30°	62.9°	3.7°	137½	8.5
35°	73.4°	4.1°	137½	8.8
40°	83.6°	4.4°	137½	9.1

[a] This energy refers to the R measurement; for A, the energy was 135½ MeV.

calculate a scattering angle, $\theta_{c.m.}$, in the center-of-mass system of the two interacting particles, and to define and calculate E_{eq}, the scattering energy equivalent to the free nucleon-nucleon scattering.

$$E_{eq}=E_{eq}'-E_s-\epsilon,$$

where E_{eq}' is the incident proton energy in a system where the target particle is at rest; E_s is the energy of the spectator particle and ϵ the binding energy of the deuteron.

A computer program was used to calculate E_{eq} and $\theta_{c.m.}$ for various values of the polar and azimuthal angles of the scattered and recoil particles and for different energies of the scattered proton. At the same time the cross sections for the quasifree events in spectator model approximation were calculated by using the free n-p and p-p cross sections at the appropriate values of E_{eq} and $\theta_{c.m.}$ and using the Hulthén wave function to obtain the momentum distribution of the nucleons within the deuteron. With these quasifree cross sections as weighting functions, $\theta_{c.m.}$ and E_{eq} were averaged over the finite geometry of the experiment (counters B and N, and the deuterium target) to obtain mean scattering angles and energies, and their rms deviations. These are listed in Table V. The experimental uncertainties on the average values of $\theta_{c.m.}$ and E_{eq} are, respectively, 1.5° and 2 MeV at all angles.

Other Spectator Model Effects

Because of the vertical and horizontal motion of the target particle in the deuteron, the plane of scattering will be tilted with respect to the plane of scattering in a system where the target particle is at rest, and the direction of $\mathbf{q}$, the momentum transfer, will be changed. Since the triple scattering parameters are defined with respect to the direction of $\mathbf{q}$, the final polarization will be an admixture of P_2, and P_1 times R, A, D, R', or A'. The contamination from these parameters will cancel to first order, if the experiment averages over the different directions of target motion with equal weighting. Second-order terms, however, will still be present, as will first-order terms to the extent that the experimental techniques bias the scattering events in favor of certain preferred directions of the target motion. Such experimental bias may be introduced, for example, by the variation with energy of N counter efficiency, by vertical misalignments of the P or N counters, or by the fact that at $\theta_2=30°$ appreciable numbers of recoil protons were stopped within the deuterium target. Errors to A and R from these effects were calculated and found to be 0.013 or less.

Differences may exist between the values of R or A at the average values of $\theta_{c.m.}$ and E_{eq} and the average values of $R(\theta_{c.m.},E_{eq})$ or $A(\theta_{c.m.},E_{eq})$ which were the quantities actually measured. In order to estimate the possible extent of such differences it is necessary to know how R and A vary with both angle and energy,

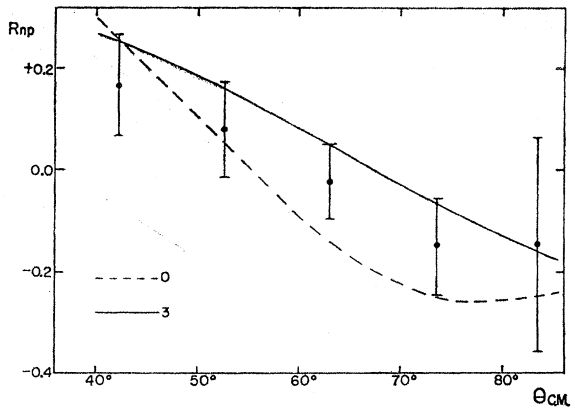

FIG. 4. Inferred value of R for free n-p scattering at 137½ MeV. The errors indicated are quadratic combinations of random and systematic errors. The curves are predictions of phase-shift solutions of Hull *et al.*, Ref. 20, at 137 MeV.

which knowledge is not yet experimentally available. An estimate of the variation of A and R was taken from the phase-shift analyses of Breit and collaborators[20] and used with the probability distribution $P(\theta_{c.m.},E_{eq})$. These calculations indicate the values of R_{p-n} at the average values of $\theta_{c.m.}$ and E_{eq} would be more negative than the experimental values by amounts ranging from 0.002 at $\theta_2=20°$ to 0.009 at $\theta_2=40°$; the values of A_{p-n} would be more negative than the experimental values by less than 0.004 at any angle. Because of the small size of these corrections and their appreciable uncertainty they have not been applied to the results quoted here.

Discussion

The spectator model neglects multiple scattering of the incident proton by the two target nucleons, final state interactions between the two target nucleons, and the ambiguity as to which of the target particles was the struck particle and which the spectator. In III, these effects are discussed, corrections are calculated (neglecting the first-mentioned effect) and estimates of the accuracy of the corrections are obtained.

In III, our quasifree p-p measurements are compared with free p-p measurements, and are seen to agree both

TABLE VI. Corrections to the spectator model, ΔR and ΔA, for quasifree p-n scattering, and values of R and A inferred for free n-p scattering. In addition to the random errors listed, there is a systematic error of $[(0.04)^2+(\frac{1}{4}\Delta R)^2]^{1/2}$ in ΔR, and hence, R (free n-p) and a systematic error of $[(0.04)^2+(\frac{1}{4}\Delta A)^2]^{1/2}$ in ΔA, and hence A (free n-p) (see text, and article III).

$\theta_{c.m.}$	ΔR	R (free n-p)	ΔA	A (free n-p)
42°	+0.140±0.039	+0.169±0.089	−0.072±0.028	−0.020±0.077
52½°	+0.086±0.025	+0.080±0.086	−0.053±0.017	+0.070±0.060
63°	+0.038±0.016	−0.023±0.065	−0.004±0.021	+0.210±0.079
73½°	+0.009±0.011	−0.151±0.090	+0.028±0.018	+0.126±0.096
83½°	+0.018±0.014	−0.146±0.207	+0.036±0.016	+0.532±0.216

[20] M. H. Hull, Jr., K. E. Lassila, H. M. Ruppel, F. A. MacDonald, and G. Breit, Phys. Rev. **122**, 1606 (1961), and private communications.

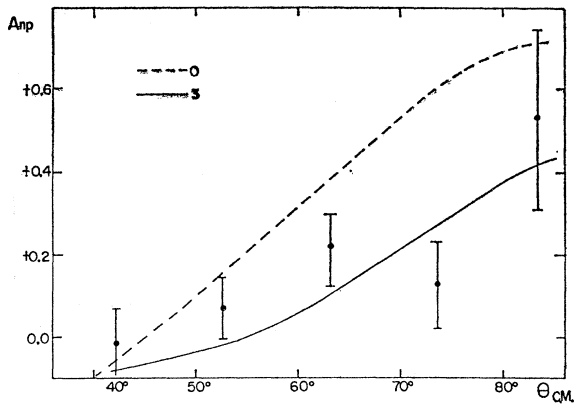

FIG. 5. Inferred value of A for free n-p scattering at 135½ MeV. The errors indicated are quadratic combinations of random and systematic errors. The curves are predictions of phase-shift solutions of Hull *et al.*, Ref. 20, at 137 MeV.

before and after the (small) correction to the spectator model is applied.

The corrections to the spectator model for quasifree p-n measurements of R and A, obtained in III, are listed in Table VI. Each correction has a random error, due to the uncertainties in averaging over the experimental resolution and to the errors on the input parameters to the theory. This random error is listed with the correction. Not listed is a systematic error of $[(0.04)^2+(\frac{1}{4}\Delta R)^2]^{1/2}$ or $[(0.04)^2+(\frac{1}{4}\Delta A)^2]^{1/2}$ due to the limited validity of the theory (see discussion in III).

Applying these corrections to our quasifree p-n results, we obtain the "free" n-p values listed in Table VI. Again, the listed errors do *not* include the systematic error.

In Figs. 4 and 5 are plotted our "free" n-p values. Here, the systematic error *has* been added, in quadrature, to the listed random error to give the error shown by the bars. Also shown in the figures are predictions of the phase-shift solutions YLAN 0 and YLAN 3 of Hull *et al.*[20] The other four solutions, YLAN 1, 2, 2M, and 3M, lie generally between the two curves shown. All solutions fit the R measurements adequately, but solutions 0, 2, and 2M fit the A measurements poorly. Solutions 3 and 3M provide the best over-all fit, and provide a very satisfactory representation of the data.

ACKNOWLEDGMENTS

We were assisted in performing these experiments by R. Koch, W. Shlaer, and P. Koehler, and in reducing the data by Miss A. Bailey and Miss N. Hubbard. Some of the techniques of the A measurement were developed in collaboration with S. Hee. We wish to thank Professor Breit and his group for supplying us with calculations based on their phase-shift solutions. Theoretical discussions with Dr. A. Cromer and Dr. A. Everett proved valuable. We are grateful to Andreas Koehler for providing us with a relatively trouble-free cyclotron, and for advising and assisting us on several technical problems.